Research Article | Vol. 27, No. 21 / 14 October 2019 / Optics Express 30225
Optics EXPRESS

Experimental demonstration of tunable graphene-polaritonic hyperbolic metamaterial

JEREMY BROUILLET,[1] GEORGIA T. PAPADAKIS,[2,*] AND AND HARRY A. ATWATER[1]

[1]*Thomas J. Watson Laboratories of Applied Physics, California Institute of Technology, California 91125, USA*
[2]*Department of Electrical Engineering, Ginzton Laboratory, Stanford University, California 94305, USA*
[*]*gpapadak@stanford.edu*

Abstract: Tuning the macroscopic dielectric response on demand holds potential for actively tunable metaphotonics and optical devices. In recent years, graphene has been extensively investigated as a tunable element in nanophotonics. Significant theoretical work has been devoted on the tuning the hyperbolic properties of graphene/dielectric heterostructures; however, until now, such a motif has not been demonstrated experimentally. Here we focus on a graphene/polaritonic dielectric metamaterial, with strong optical resonances arising from the polar response of the dielectric, which are, in general, difficult to actively control. By controlling the doping level of graphene via external bias we experimentally demonstrate a wide range of tunability from a Fermi level of $E_F = 0$ eV to $E_F = 0.5$ eV, which yields an effective epsilon-near-zero crossing and tunable dielectric properties, verified through spectroscopic ellipsometry and transmission measurements.

1. Introduction

Spectral tunability is key for controlling light-matter interactions, critical for many applications including emission control, surface enhanced spectroscopy, sensing, and thermal control. Particularly in the subwavelength range, tuning plasmonic resonances has been essential in controlling color, typically achieved by controlling the size of plasmonic nanoparticles, antennas and metamaterials [1–4]. In obtaining a large range of spectral tunability, it is preferable to operate near an optical resonance rather than a broadband plasmonic response. Nevertheless, it is in general easier to tune a broadband optical response rather than a resonant one since resonances in nanophotonics typically entail subwavelength-scale geometrical features.

From a very wide range of recently investigated metamaterials and heterostructures for spectral control, particular emphasis has been given to hyperbolic media, due to enhanced light-matter interactions arising from a larger range of wavenumbers available for propagating modes [5]. This property makes hyperbolic media attractive as hyperlenses, broadband thermal emitters, perfect absorbers, among others. These media are in generally uniaxial and support a hyperbolic frequency dispersion given by the equation [3,6–8]

$$\frac{k_x^2 + k_y^2}{\epsilon_e} + \frac{k_z^2}{\epsilon_o} = \frac{\omega^2}{c^2} \tag{1}$$

where ϵ_o and ϵ_e refer to the ordinary (in-plane) and extraordinary (out-of-plane) dielectric permittivity, respectively. Due to the different sign in ϵ_o and ϵ_e, upon fixing the frequency ω, the isofrequency diagram of the relevant electromagnetic modes opens up into a hyperbola, giving rise to a very large density of optical states, promising for waveguiding [9], emission engineering and Purcell enhancement [1,2,10] thermal photonics [11], lasing [12], and imaging [13,14]. Particularly, near the epsilon-near-zero frequency crossing of either ϵ_o or ϵ_e, many

#372223 https://doi.org/10.1364/OE.27.030225
Journal © 2019 Received 10 Jul 2019; revised 11 Sep 2019; accepted 17 Sep 2019; published 4 Oct 2019

Optics EXPRESS

exciting phenomena can be supported, the most prominent of which is light propagation with near-zero phase advance [15–17].

There has been significant effort in frequency-tuning of the optical response of hyperbolic metamaterials [6,18–21]. For this, particular interest holds the case of graphene, a well-studied monolayer material for electronics [22] and in infrared photonics [23]. Namely, the optical properties of graphene can be dynamically tuned via optical pumping [24], or with electrostatic modulation of its carrier concentration with field-effect gating [25,26], often targeting tunable plasmonic properties [27–29]. The high degree of localization of graphene plasmons, together with the dielectric tunability of graphene provides a promising platform for investigating tunable graphene-based hyperbolic metamaterials. There has already been considerable theoretical effort in the past decade to understand the properties of tunable graphene metamaterials [30–34], with significant focus on the potential of tuning hyperbolic properties of graphene/dielectric planar heterostructures [6,35–38]. There have previously been experimental demonstrations of graphene-based hyperbolic media [39,40], nevertheless, the reported properties have remained fixed at the time of fabrication. No post-fabrication way to control the dielectric permittivity tensor (ϵ_o and ϵ_e in Eq. (1)) has been reported until now. In this work, we experimentally demonstrate large dynamical tuning ratio of the dielectric response of a graphene-based hyperbolic metamaterial.

Gating graphene, when integrated with dielectric layers, is difficult due to graphene's two-dimensional nature with weak out-of-plane Van der Waals bonds that yield poor adhesion to most dielectric substrates. Furthermore, large-area graphene sheets on the order of few mm^2 with gate-induced tunability are needed to perform metamaterial optical measurements at infrared frequencies. Exfoliated flakes are generally limited to sizes of tens of μm^2, so large-area graphene samples grown by chemical vapor deposition and subsequently transferred from their growth substrates, are necessary. Additionally, deposition of large-area thin dielectric layers on graphene is challenging. Films prepared by electron-beam evaporation exhibit thermal stress-induced delamination [41]. Films grown by atomic layer deposition (ALD) with an H_2O precursors exhibit difficulty in bonding to chemically-inert hydrophobic graphene [42], whereas ozone-based ALD processes oxidize graphene.

Here, we discuss how we overcome these challenges and are, thus, able to tune a graphene-based hyperbolic metamaterial unit cell for a wide range of doping levels in graphene translating to a Fermi level that ranges from $E_F = 0$ eV to $E_F = 0.5$ eV, without dielectric breakdown. Previous theoretical proposals have considered non-dispersive dielectric materials [6,35–37], thereby yielding a broadband hyperbolic response. By contrast, here, we consider a polaritonic dielectric material, namely SiO_2. The polaritonic resonances that all polar materials exhibit at infrared frequencies, at their Reststrahlen band, are typically not tunable, as they constitute a fundamental material property. Furthermore, resonances in nanophotonics are typically induced via subwavelength photonic structures, which are also quite difficult to dynamically tune. We show here that, upon the integration of graphene, it is feasible to actively tune the polaritonic resonances of naturally occuring dielectrics. Graphene provides a tunable character to the in-plane response of the composite graphene/SiO_2 heterostructure, and its plasmonic nature assigns a hyperbolic frequency region near the polar resonance of SiO_2, at a free-space wavelength of 20 μm. We are therefore able to experimentally observe, through multi-angle spectroscopic ellipsometry and transmittance measurements, a tunable epsilon-near zero permittivity along the in-plane direction near the surface phonon polaritonic resonance while leaving the out-of-plane response unchanged (due to the two-dimensional nature of graphene), thereby yielding a widely tunable hyperbolic response.

Optics EXPRESS

2. Metamaterial motif and experimental realization

The metamaterial under consideration is depicted in Fig. 1, and is composed of a graphene monolayer sandwitched in between two SiO_2 layers of thickness 300 nm. The alumina (Al_2O3) layers depicted in Fig. 1 have thickness thickness 0.5 nm and are placed to prevent poor graphene adhesion. Particularly, a viable dielectric deposition method was developed consisting of functionalization of the surface by deposition of trimethylaluminium (TMA) [43] or an aluminum nucleation layer [44] to create a seed layer for additional deposition. A suitably thin layer of aluminum is needed so that it can fully oxidize and not compromise the electrical gating of the graphene. We found that deposition of AL_2O_3 via plasma-enhanced chemical vapor deposition (PECVD) resulted in reduced thermal stress and avoided delamination. The graphene is grown by chemical vapor deposition (CVD) and transferred onto the thermal oxide, whereas the top SiO_2 film is deposited by plasma-enhanced chemical vapor deposition (PECVD). The thickness of the film layers were measured by both a thin film analyzer and visible ellipsometry with a qualitative agreement of 2nm. Lithographically-defined patterns were used to deposit 3nm/100nm of Cr/Au contacts on the graphene layer, and were used to gate the graphene monolayer against the silicon substrate, which serves as the back-side contact for field-effect tuning.

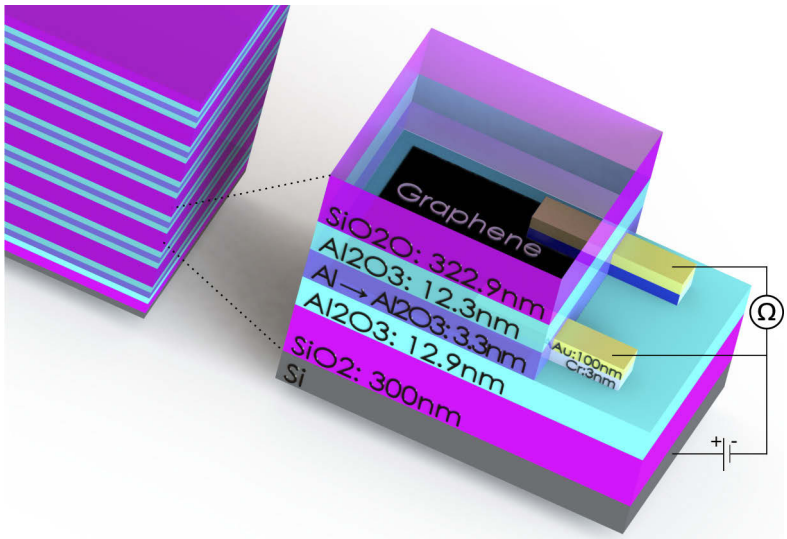

Fig. 1. Left: Schematic of a theoretical metamaterial stack. Right: Schematic of the fabricated individual device. The layers: Lightly-doped silicon substrate, thermally-grown SiO2, Al_2O_3, transferred chemical-vapor deposited (CVD) graphene, Al_2O_3, and plasma-enhance chemical vapor deposition SiO_2. The thin layers of Al_2O_3 are necessary for the feasibility of the fabrication. The thick SiO_2 contribute to the majority of the dielectric response. Contacts are added to gate and measure the resistance of the graphene. The graphene is tuned by gating against the back silicon substrate.

3. Theory and modeling

Since the composite in Fig. 1 is extremely subwavelength to infrared light, one can homogenize it and assign an effective in-plane and out-of-plane dielectric response, namely ϵ_o and ϵ_e [8]. The two-dimensional nature of graphene leaves the out-of-plane response unaffected, therefore in the out-of-plane direction, this metamaterial behaves to far-field radiation effectively as bulk SiO_2. By striking contrast, by electrostatically tuning the graphene carrier we can shift the

Optics EXPRESS

epsilon-near-zero point of ϵ_o, and therefore control the hyperbolicity of the heterostructure as shown in Fig. 2.

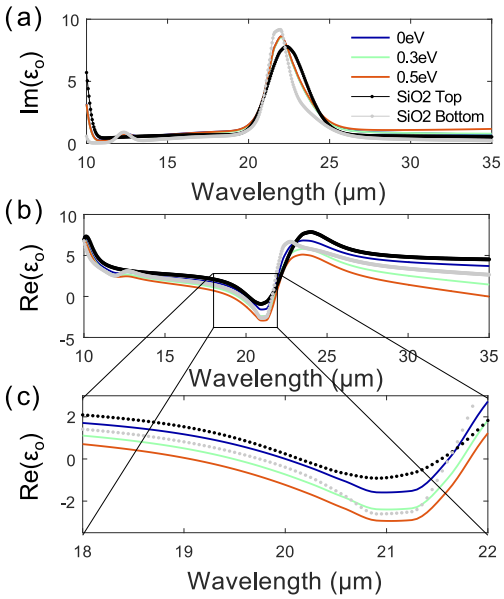

Fig. 2. Ellipsometrically derived effective in-plane dielectric permittivity, ϵ_o, for the graphene/SiO_2 metamaterial of Fig. 1, under applied bias, for three different Fermi levels $E_F = 0$ eV, $E_F = 0.3$ eV, $E_F = 0.5$ eV. Grey and black curves correspond to the homogeneous dielectric permittivity of the bottom and top SiO_2 films, respectively. (a) Imaginary part, and (b) real part. (c) Inset showing the epsilon-near-zero regime of ϵ_o at different E_F's.

In estimating the Fermi level to which we can actively tune the doping level in graphene, we use a capacitor model based on the materials between the gate and the applied voltage [45].

$$E_f = 0.031\sqrt{V - V_{\text{Dirac}}}. \tag{2}$$

Experimentally, the location of the Dirac peak was determined via measuring change in sheet resistance. Furthermore, we use the Kubo formula [46] calculate the sheet conductance σ from the E_f of graphene. This value can be used to compute the transfer matrix for graphene [47].

$$\overleftrightarrow{G} = \begin{bmatrix} 1 & 0 \\ 4\pi\sigma/c & 0 \end{bmatrix} \tag{3}$$

We utilize the transfer matrix approach [48], accounting for graphene via $\overleftrightarrow{G}$, and obtain the complex scattering amplitudes of the fields at different Fermi levels E_F. In these calculations, fabrication and material imperfections are removed by having, a priori, measured experimentally the individual layer thicknesses and optical constants of all thin films in the metamaterial, with ellipsometry. For example, in Fig. 2(a) and (b) we show the experimentally determined dielectric permittivity of the top and bottom SiO_2 films shown in Fig. 1, where their small differences are are expected since the top SiO_2 is deposited via PECVD whereas the bottom one is thermally grown. The scattering amplitudes are fed into previously developed parameter retrieval approaches [8], from which we obtain an effective uniaxial tensorial dielectric permittivity $\epsilon = \text{diag}(\epsilon_o, \epsilon_o, \epsilon_e)$ that characterizes the metamaterial composite. This process is repeated at different gating voltages V, in other words for different Fermi levels E_F.

Optics EXPRESS

4. Results

By taking spectroscopic ellipsometry measurements of the full metamaterial stack of Fig. 1, we perform an ellipsometric fitting where we use the effective dielectric permittivity $\epsilon = \text{diag}(\epsilon_o, \epsilon_o, \epsilon_e)$ as a model to fit to the experimental data, namely the ellipsometric observables Ψ and Δ. In Fig. 2(a) and (b) we show the imaginary and real part of the ellipsometrically-derived in-plane permittivity ϵ_o, at different Fermi levels E_F. We note that the out-of-plane effective permittivity ϵ_e is not tunable as described above, and therefore is omitted. There resonant character of ϵ_o near the regime of 20 μm is attributed to the surface phonon polaritonic resonance of SiO_2 at this wavelength, nevertheless this resonance has now become tunable via incorporation of a monolayer-thick graphene sheet in between SiO_2 films. As can be clearly seen in 2(c), by gradually tuning the Fermi level of graphene from $E_F = 0$ eV (blue curves) to $E_F = 0.3$ eV (green curves) to $E_F = 0.5$ eV, we redshift the infrared response of the metamaterial by approximately a micron, i.e. from a near-zero crossing at 20 μm under no bias to 19 μm under large applied bias. Redshifting is expected as a response of applied bias because the electrostatic doping induces

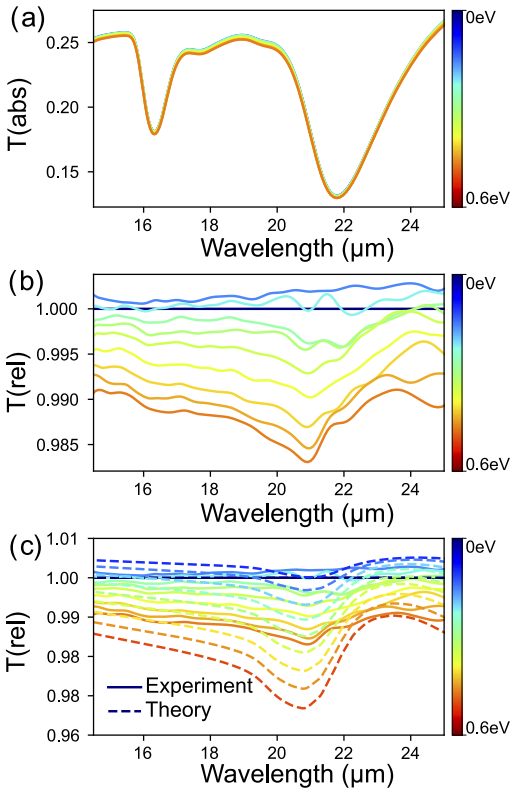

Fig. 3. (a) Absolute FTIR transmission measurements over a range of Fermi levels from $E_F = 0$ eV to $E_F = 0.6$ eV. (b) Experimental data normalized to E_F=0, the Dirac point of graphene, in order to empasize the gate-tunable response of the metamaterial. (c) Experiment compared with theory. The theoretical results were computed using the ellipsometrilly derived dielectric properties of the metamaterial, and the experimentally measured thicknesses of each constituent layer. Data are normalized to the case of E_F=0, similar to panel (b). Deviations between theory and experiment arise due to hysteresis of the graphene induced by charge trapping.

Optics EXPRESS

additional charge carriers in the graphene sheet, hence making the composite medium more metallic.

In addition to spectroscopic ellipsometry, we perform Fourier-transform infrared spectroscopy (FTIR) to measure the sample transmission, and compare with the results of spectroscopic ellipsometry shown above, derived based on initial parameter retrieval-based derivation of $\epsilon = \mathrm{diag}(\epsilon_o, \epsilon_o, \epsilon_e)$. Electrostatically gating the graphene induces changes in the transmission of the composite metamaterial, as shown in Fig. 3. Namely, as mentioned above, gating the graphene monolayer makes the composite metamaterial more metallic and, therefore, less transmissive, as shown with the colormap in Figs. 3(b) and (c). The dips near the wavelengths of 16 μm and 20 μm correspond to the two surface phonon polariton resonances of SiO_2, where the material absorbs resonantly, resulting in low transmittance. We note that, experimentally, graphene exhibits hysteresis, which is attributed to defects induced by the deposition of the aluminum layer, resulting in the discrepancies between experiment and theory. As the graphene is tuned, the Dirac peak shifts in the direction of applied bias, causing the sample to experience a reduced E_f, giving qualitative experimental agreement with theory without fitting parameters as can be seen in Fig. 3(c).

To further illustrate the epsilon-near-zero shifting and the resonant nature of the in-plane dielectric response of this metamaterial, i.e. ϵ_o, in Fig. 4 we show the relative change in dielectric permittivity, i.e. $\Delta\epsilon = 100 \times (\epsilon_{o,V=0} - \epsilon_{o,V})/\epsilon_{o,V=0}$, for two different applied bias corresponding to $E_{F=0.2}$ eV and to $E_{F=0.4}$ eV, with blue and red color, respectively. These calculations were performed using the experimentally derived values for the optical properties and thicknesses of the constitutive components of the metamaterial, as described above. Near the surface phonon resonance of SiO_2 at 20 μm, significant tuning of the real part of ϵ_o is observed, coming from the epsilon-near-zero tuning, which shifts by approximately 1 micron. Bearing in mind that the out-of-plane response of this metamaterial (ϵ_e in Eq. (1)) is not tunable due to the two-dimensional nature of graphene, as explained above, the change in sign of ϵ_o on the left axis in Fig. 4 corresponds to a topological transition of the isofrequency surface of this metamaterial.

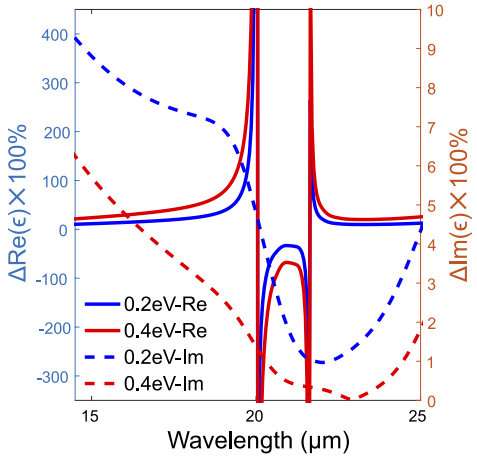

Fig. 4. Relative change of the effective in-plane dielectric permittivity, ϵ_o, of the metamaterial, for two different Fermi levels, namely $E_F = 0.2$ eV (blue curves) and $E_F = 0.4$ eV (red curves), with respect to the case $E_F = 0$ eV. Solid curves (left y-axis) correspond to real parts and dashed curves correspond to imaginary parts (right y-axis).

Optics EXPRESS

5. Conclusions

In summary, we have experimentally demonstrated a graphene/polaritonic dielectric metamaterial with tunable epsilon-near-zero permittivity response. By tuning the Fermi level of graphene by 0.5 eV, we observe a shift of 1 μm in the near-zero response. Although previous theoretical proposals have focused on non-dispersive dielectric materials between graphene monolayers, here we showed that utilizing the polar response of dielectrics at infrared frequencies benefits tunability, and additionally provides means of tuning constitutive material properties of polar dielectrics and semiconductors, by incorporating graphene. Ellipsometry was used to determine the optical properties (dielectric response and thickness) of the constituent materials, and, based on effective parameter retrievals that homogenize the metamaterial, we experimentally characterized the full metamaterial stack. FTIR transmission measurements agree with our ellipsometric results, where transmission reduction is directly attributed to electrostatically induced charges in graphene and to epsilon-near-zero tuning.

Funding

National Science Foundation (1144469, Graduate Research Fellowship); TomKat Center for Sustainable Energy, Stanford University.

Disclosures

The authors declare that there are no conflicts of interest related to this article.

References

1. D. Lu, J. J. Kan, E. E. Fullerton, and Z. Liu, "Enhancing spontaneous emission rates of molecules using nanopatterned multilayer hyperbolic metamaterials," Nat. Nanotechnol. **9**(1), 48–53 (2014).
2. J. Zhou, A. F. Kaplan, L. Chen, and L. J. Guo, "Experiment and theory of the broadband absorption by a tapered hyperbolic metamaterial array," ACS Photonics **1**(7), 618–624 (2014).
3. Z. Jacob, J.-Y. Kim, G. V. Naik, A. Boltasseva, E. E. Narimanov, and V. M. Shalaev, "Engineering photonic density of states using metamaterials," Appl. Phys. B **100**(1), 215–218 (2010).
4. J. A. Schuller, E. S. Barnard, W. Cai, Y. C. Jun, J. S. White, and M. L. Brongersma, "Plasmonics for extreme light concentration and manipulation," Nat. Mater. **9**(3), 193–204 (2010).
5. D. R. Smith, W. J. Padilla, D. Vier, S. C. Nemat-Nasser, and S. Schultz, "Composite medium with simultaneously negative permeability and permittivity," Phys. Rev. Lett. **84**(18), 4184–4187 (2000).
6. A. Poddubny, I. Iorsh, P. Belov, and Y. Kivshar, "Hyperbolic metamaterials," Nat. Photonics **7**(12), 948–957 (2013).
7. D. Smith and D. Schurig, "Electromagnetic wave propagation in media with indefinite permittivity and permeability tensors," Phys. Rev. Lett. **90**(7), 077405 (2003).
8. G. T. Papadakis, P. Yeh, and H. A. Atwater, "Retrieval of material parameters for uniaxial metamaterials," Phys. Rev. B **91**(15), 155406 (2015).
9. V. E. Babicheva, "Long-range propagation of plasmon and phonon polaritons in hyperbolic-metamaterial waveguides," J. Opt. **19**(12), 124013 (2017).
10. C. L. Cortes, M. Otten, and S. K. Gray, "Ground-state cooling enabled by critical coupling and dark entangled states," Phys. Rev. B **99**(1), 014107 (2019).
11. S.-A. Biehs, M. Tschikin, and P. Ben-Abdallah, "Hyperbolic metamaterials as an analog of a blackbody in the near field," Phys. Rev. Lett. **109**(10), 104301 (2012).
12. A. Fang, T. Koschny, and C. M. Soukoulis, "Lasing in metamaterial nanostructures," J. Opt. **12**(2), 024013 (2010).
13. Z. Liu, H. Lee, Y. Xiong, C. Sun, and X. Zhang, "Far-field optical hyperlens magnifying sub-diffraction-limited objects," Science **315**(5819), 1686 (2007).
14. D. S. Weile, "Electromagnetic metamaterials: Physics and engineering explorations (engheta, n. and ziolkowski, rw; 2006)[book review]," IEEE Antennas Propag. Mag. **49**(4), 137–139 (2007).
15. R. Maas, J. Parsons, N. Engheta, and A. Polman, "Experimental realization of an epsilon-near-zero metamaterial at visible wavelengths," Nat. Photonics **7**(11), 907–912 (2013).
16. A. M. Mahmoud and N. Engheta, "Wave–matter interactions in epsilon-and-mu-near-zero structures," Nat. Commun. **5**(1), 5638 (2014).
17. N. Engheta, "Pursuing near-zero response," Science **340**(6130), 286–287 (2013).
18. G. T. Papadakis and H. A. Atwater, "Field-effect induced tunability in hyperbolic metamaterials," Phys. Rev. B **92**(18), 184101 (2015).

Optics EXPRESS

19. J. A. Roberts, S.-J. Yu, P.-H. Ho, S. Schoeche, A. L. Falk, and J. A. Fan, "Tunable hyperbolic metamaterials based on self-assembled carbon nanotubes," Nano Lett. **19**(5), 3131–3137 (2019).
20. L. Lu, R. E. Simpson, and S. K. Valiyaveedu, "Active hyperbolic metamaterials: progress, materials and design," J. Opt. **20**(10), 103001 (2018).
21. C. Shi, X. He, J. Peng, G. Xiao, F. Liu, F. Lin, and H. Zhang, "Tunable terahertz hybrid graphene-metal patterns metamaterials," Opt. Laser Technol. **114**, 28–34 (2019).
22. K. S. Novoselov, A. K. Geim, S. Morozov, D. Jiang, M. Katsnelson, I. Grigorieva, S. Dubonos, and A. A. Firsov, "Two-dimensional gas of massless dirac fermions in graphene," Nature **438**(7065), 197–200 (2005).
23. D. R. Andersen, "Graphene-based long-wave infrared tm surface plasmon modulator," J. Opt. Soc. Am. B **27**(4), 818–823 (2010).
24. V. Ryzhii, M. Ryzhii, and T. Otsuji, "Negative dynamic conductivity of graphene with optical pumping," J. Appl. Phys. **101**(8), 083114 (2007).
25. A. Vakil and N. Engheta, "Transformation optics using graphene," Science **332**(6035), 1291–1294 (2011).
26. M. Polini, R. Asgari, G. Borghi, Y. Barlas, T. Pereg-Barnea, and A. MacDonald, "Plasmons and the spectral function of graphene," Phys. Rev. B **77**(8), 081411 (2008).
27. E. Hwang and S. D. Sarma, "Dielectric function, screening, and plasmons in two-dimensional graphene," Phys. Rev. B **75**(20), 205418 (2007).
28. V. W. Brar, M. S. Jang, M. Sherrott, J. J. Lopez, and H. A. Atwater, "Highly confined tunable mid-infrared plasmonics in graphene nanoresonators," Nano Lett. **13**(6), 2541–2547 (2013).
29. X. He, F. Liu, F. Lin, G. Xiao, and W. Shi, "Tunable MoS2 modified hybrid surface plasmon waveguides," Nanotechnology **30**(12), 125201 (2019).
30. J. Linder and K. Halterman, "Graphene-based extremely wide-angle tunable metamaterial absorber," Sci. Rep. **6**(1), 31225 (2016).
31. A. Andryieuski and A. V. Lavrinenko, "Graphene metamaterials based tunable terahertz absorber: effective surface conductivity approach," Opt. Express **21**(7), 9144–9155 (2013).
32. H. Xiong, Y.-B. Wu, J. Dong, M.-C. Tang, Y.-N. Jiang, and X.-P. Zeng, "Ultra-thin and broadband tunable metamaterial graphene absorber," Opt. Express **26**(2), 1681–1688 (2018).
33. S. Zainud-Deen, A. Mabrouk, and H. Malhat, "Frequency tunable graphene metamaterial reflectarray," *2017 XXXIInd General Assembly and Scientific Symposium of the International Union of Radio Science (URSI GASS)* pp. 1–4, (2017).
34. A. Al Sayem, A. Shahriar, M. Mahdy, and M. S. Rahman, "Control of reflection through epsilon near zero graphene based anisotropic metamaterial," *8th International Conference on Electrical and Computer Engineering* pp. 812–815 (2014).
35. I. V. Iorsh, I. S. Mukhin, I. V. Shadrivov, P. A. Belov, and Y. S. Kivshar, "Hyperbolic metamaterials based on multilayer graphene structures," Phys. Rev. B **87**(7), 075416 (2013).
36. M. A. Othman, C. Guclu, and F. Capolino, "Graphene–dielectric composite metamaterials: evolution from elliptic to hyperbolic wavevector dispersion and the transverse epsilon-near-zero condition," J. Nanophotonics **7**(1), 073089 (2013).
37. B. Janaszek, A. Tyszka-Zawadzka, and P. Szczepański, "Tunable graphene-based hyperbolic metamaterial operating in sclu telecom bands," Opt. Express **24**(21), 24129–24136 (2016).
38. S. Achilli, E. Cavaliere, T. H. Nguyen, M. Cattelan, and S. Agnoli, "Growth and electronic structure of 2d hexagonal nanosheets on a corrugated rectangular substrate," Nanotechnology **29**(48), 485201 (2018).
39. Y.-C. Chang, C.-H. Liu, C.-H. Liu, S. Zhang, S. R. Marder, E. E. Narimanov, Z. Zhong, and T. B. Norris, "Realization of mid-infrared graphene hyperbolic metamaterials," Nat. Commun. **7**(1), 10568 (2016).
40. S. Dai, Q. Ma, M. K. Liu, T. Andersen, Z. Fei, M. D. Goldflam, M. Wagner, K. Watanabe, T. Taniguchi, M. Thiemens, F. Keilmann, G. C. A. M. Janssen, S.-E. Zhu, P. Jarillo-Herrero, M. M. Fogler, and D. N. Basov, "Graphene on hexagonal boron nitride as a tunable hyperbolic metamaterial," Nat. Nanotechnol. **10**(8), 682–686 (2015).
41. D. Q. McNerny, B. Viswanath, D. Copic, F. R. Laye, C. Prohoda, A. C. Brieland-Shoultz, E. S. Polsen, N. T. Dee, V. S. Veerasamy, and A. J. Hart, "Direct fabrication of graphene on sio 2 enabled by thin film stress engineering," Sci. Rep. **4**(1), 5049 (2014).
42. J. S. Park, K. D. Kihm, H. Kim, G. Lim, S. Cheon, and J. S. Lee, "Wetting and evaporative aggregation of nanofluid droplets on cvd-synthesized hydrophobic graphene surfaces," Langmuir **30**(28), 8268–8275 (2014).
43. B. Lee, G. Mordi, M. Kim, Y. Chabal, E. Vogel, R. Wallace, K. Cho, L. Colombo, and J. Kim, "Characteristics of high-k al 2 o 3 dielectric using ozone-based atomic layer deposition for dual-gated graphene devices," Appl. Phys. Lett. **97**(4), 043107 (2010).
44. S. Kim, J. Nah, I. Jo, D. Shahrjerdi, L. Colombo, Z. Yao, E. Tutuc, and S. K. Banerjee, "Realization of a high mobility dual-gated graphene field-effect transistor with al 2 o 3 dielectric," Appl. Phys. Lett. **94**(6), 062107 (2009).
45. I. J. Luxmoore, C. H. Gan, P. Q. Liu, F. Valmorra, P. Li, J. Faist, and G. R. Nash, "Strong coupling in the far-infrared between graphene plasmons and the surface optical phonons of silicon dioxide," ACS Photonics **1**(11), 1151–1155 (2014).
46. L. Falkovsky, "Optical properties of graphene," J. Phys.: Conf. Ser. **129**, 012004 (2008).
47. G. T. Papadakis, "Optical response in planar heterostructures: From artificial magnetism to angstrom-scale metamaterials," Ph.D. thesis, California Institute of Technology (2018).
48. A. Pochi Yeh, "Optical waves in layered media," (1988).